Oxidation and Glycolytic Cleavage of Etheno and Propano DNA Base Adducts[†]

Charles G. Knutson,[‡] Emily H. Rubinson,[‡] Dapo Akingbade,[‡] Carolyn S. Anderson,[§] Donald F. Stec,[§] Katya V. Petrova,[§] Ivan D. Kozekov,[§] F. Peter Guengerich,[‡] Carmelo J. Rizzo,[§] and Lawrence J. Marnett*[,‡,§,||]

A. B. Hancock Jr. Memorial Laboratory for Cancer Research, Departments of Biochemistry, Chemistry, and Pharmacology, Vanderbilt Institute of Chemical Biology, Center in Molecular Toxicology, Vanderbilt-Ingram Cancer Center, Vanderbilt University School of Medicine, Nashville, Tennessee 37232-0146

Received August 31, 2008; Revised Manuscript Received November 25, 2008

ABSTRACT: Non-invasive strategies for the analysis of endogenous DNA damage are of interest for the purpose of monitoring genomic exposure to biologically produced chemicals. We have focused our research on the biological processing of DNA adducts and how this may impact the observed products in biological matrixes. Preliminary research has revealed that pyrimidopurinone DNA adducts are subject to enzymatic oxidation in vitro and in vivo and that base adducts are better substrates for oxidation than the corresponding 2′-deoxynucleosides. We tested the possibility that structurally similar exocyclic base adducts may be good candidates for enzymatic oxidation in vitro. We investigated the in vitro oxidation of several endogenously occurring etheno adducts [1,N^2-ε-guanine (1,N^2-ε-Gua), N^2,3-ε-Gua, heptanone-1,N^2-ε-Gua, 1,N^6-ε-adenine (1,N^6-ε-Ade), and 3,N^4-ε-cytosine (3,N^4-ε-Cyt)] and their corresponding 2′-deoxynucleosides. Both 1,N^2-ε-Gua and heptanone-1,N^2-ε-Gua were substrates for enzymatic oxidation in rat liver cytosol; heteronuclear NMR experiments revealed that oxidation occurred on the imidazole ring of each substrate. In contrast, the partially or fully saturated pyrimidopurinone analogues [i.e., 5,6-dihydro-M_1G and 1,N^2-propanoguanine (PGua)] and their 2′-deoxynucleoside derivatives were not oxidized. The 2′-deoxynucleoside adducts, 1,N^2-ε-dG and 1,N^6-ε-dA, underwent glycolytic cleavage in rat liver cytosol. Together, these data suggest that multiple exocyclic adducts undergo oxidation and glycolytic cleavage in vitro in rat liver cytosol, in some instances in succession. These multiple pathways of biotransformation produce an array of products. Thus, the biotransformation of exocyclic adducts may lead to an additional class of biomarkers suitable for use in animal and human studies.

Oxidative stress induces cellular damage that contributes to the onset of multiple diseases, including cancer (*1, 2*). Reactive oxygen and nitrogen species produced from the immune response and during cellular respiration (occasions of oxidative stress) initiate the modification and breakdown of cellular macromolecules, including polyunsaturated lipids and DNA. Products of lipid and DNA peroxidation (principally α,β-unsaturated aldehydes) also react with DNA to produce etheno, propano, and pyrimidopurinone DNA base adducts. A growing body of evidence suggests that endogenous DNA lesions are involved in the development of cancer (*3, 4*). Therefore, the quantification of DNA adducts as biomarkers of oxidative stress may be useful for clinical and population-based risk assessment studies (*5, 6*). Non-invasive strategies for the analysis of adducts (i.e., quantifying urinary adduct levels) comprise an attractive approach for biomarker acquisition and detection, and several laboratories have implemented this strategy (*7, 8*).

Our laboratory is investigating biological factors (i.e., enzymatic oxidation, biliary elimination, etc.) that may limit the analysis of endogenously produced DNA adducts in urine. The pyrimidopurinone adduct, M_1dG[1] [3-(2′-deoxy-β-D-*erythro*-pentofuranosyl)pyrimido[1,2-α]purin-10(3*H*)-one], has been the focus of several investigations (*9–12*). M_1dG is derived from dG in reactions with either MDA (product of lipid peroxidation and prostaglandin synthesis) or base propenal (product of DNA peroxidation) (*13–19*) and is miscoding in bacteria and humans (*20, 21*). Genetic and biochemical evidence suggests that M_1dG is released from DNA by nucleotide excision repair (*20, 22*), which leads to the release of the 2′-deoxynucleoside (M_1dG) from cells (*23*). We recently described the biological processing of free M_1dG and the base adduct, M_1G (*9–12*). M_1dG undergoes a single oxidation at the 6-position of the pyrimido ring to 6-oxo-

[†] C.G.K. was supported by U.S. Public Health Service Grant T32 ES007028. This work was supported by Research Grants CA87819 (L.J.M.), R01 ES010546 (F.P.G.), and ES05355 (C.J.R.) and Center Grant ES000267 from the National Institutes of Health.

* To whom correspondence should be addressed. E-mail: larry.marnett@vanderbilt.edu. Phone: (615) 343-7329. Fax: (615) 343-7534.

[‡] Department of Biochemistry, Vanderbilt University School of Medicine.

[§] Department of Chemistry, Vanderbilt University.

[||] Department of Pharmacology, Vanderbilt University School of Medicine.

[1] Abbreviations: M_1dG, 3-(2′-deoxy-β-D-*erythro*-pentofuranosyl)pyrimido[1,2-α]purin-10(3*H*)-one; M_1G, pyrimido[1,2-α]purin-10(3*H*)-one; dG, 2′-deoxyguanosine; 1,N^2-ε-Gua, 1,N^2-ethenoguanine; N^2,3-ε-Gua, N^2,3-ethenoguanine; 1,N^6-ε-Ade, 1,N^6-ethenoadenine; 3,N^4-ε-Cyt, 3,N^4-ethenocytosine; heptanone-1,N^2-ε-Gua, 7-(2-oxoheptyl)-1,N^2-ethenoguanine; PNP, purine nucleoside phosphorylase; 5,6-dihydro-M_1dG, 3-(2′-deoxy-β-D-*erythro*-pentofuranosyl)-5,6-dihydropyrimido[1,2-α]purin-10-(3*H*)-one; PGua, 1,N^2-propanoguanine; dIno, 2′-deoxyinosine; AO, aldehyde oxidase; XO, xanthine oxidase; XOR, xanthine oxidoreductase; PNP, purine nucleoside phosphorylase; MDA, malondialdehyde.

10.1021/bi801654j CCC: $40.75
Published on Web 01/08/2009

M_1dG, whereas M_1G undergoes successive oxidations: first at the 6-position of the pyrimido ring and then at the 2-position of the imidazole ring to produce 6-oxo-M_1G and 2,6-dioxo-M_1G, respectively. Comparing the turnover of M_1dG, M_1G, and 6-oxo-M_1G in rat liver cytosol demonstrated that the bases were better substrates for oxidation than the 2′-deoxynucleoside (~5-fold).

Although no DNA glycosylases have been implicated in the release of M_1G from DNA, several structurally similar etheno adducts (1,N^2-ε-Gua, N^2,3-ε-Gua, 1,N^6-ε-Ade, and 3,N^4-ε-Cyt) are reported substrates for DNA glycosylases (*24–28*). Due to the higher apparent rate of turnover of the M_1G bases, and the structural similarity of etheno adducts, we hypothesized that etheno DNA base adducts would be likely to undergo oxidation, with the imidazole ring being a probable target for oxidation. In addition, we investigated several analogues of M_1dG to probe for structural requirements leading to the oxidation of exocyclic adducts.

EXPERIMENTAL PROCEDURES

Chemicals and Reagents. All chemicals were obtained from commercial sources and used as received. Solvents were of HPLC grade purity or higher. M_1dG (*29*), 6-oxo-M_1dG (*12*), 5,6-dihydro-M_1dG (*30*), PdG (*31*), 1,N^2-ε-Gua (*32*), N^2,3-ε-Gua (*32*), heptanone-1,N^2-ε-dG (*33*), 1,N^6-ε-Ade (*34*), and 3,N^4-ε-dC (*35*) were synthesized as previously described. Liver cytosols were prepared by established methods (*36*). Bovine XO from buttermilk was obtained from CalBiochem (La Jolla, CA). PNP was purchased from Sigma (St. Louis, MO). HPLC separations were performed on a Waters 2695 autosampler and binary pump with a Waters 2487 dual wavelength UV detector. LC−MS/MS and LC−MS^n spectra were recorded on either ThermoElectron Quantum or LTQ instruments.

Heptanone-1,N^2-ε-Gua Synthesis. Heptanone-1,N^2-ε-dG (12.3 mg, 0.03 mmol) was dissolved in 1 M HCl (4 mL) and stirred at 65−70 °C for 3 h. The reaction mixture was neutralized with 1 N NaOH and lyophilized. The resulting solid was dissolved in DMSO and purified by HPLC to afford heptanone-1,N^2-ε-Gua (4.1 mg, 47% yield) as a white solid. The purity of the product was judged to be >98% by HPLC: ^{1}H NMR (600 MHz, DMSO-d_6) δ 12.39 (br s, 2H), 7.84 (br s, 1H), 7.07 (s, 1H), 4.10 (s, 2H), 2.55 (t, 2H), 1.49 (m, 2H), 1.25 (m, 4H), 0.85 (t, 3H); positive ESI-MS *m*/*z* 288 $[M + H]^+$; MS/MS of *m*/*z* 288 (sid = 10, collision energy, 45 eV) *m*/*z* (relative intensity) 288 (12), 260 (8) 190 (100) 152 (4); ^{13}C NMR (150 MHz, DMSO-d_6) δ 206.1, 154.3, 151.4, 147.3, 137.4, 117.8, 116.0, 115.7, 70.2, 41.6, 31.3, 23.1, 22.4, 14.3; FAB HRMS *m*/*z* calculated for $C_{14}H_{18}N_5O_2$ (M + H) 288.1460, found 288.1460.

Chromatography Methods. **Method A.** Samples were separated on a Phenomenex Luna C18(2) column (4.6 mm × 250 mm, 5 μm) equilibrated with 95% solvent A (0.5% formic acid in H_2O) and 5% solvent B (0.5% formic acid in methanol) at a flow rate of 1 mL/min. The solvent was programmed as follows: a linear gradient from the starting solvent to 30% B in 15 min, increasing to 80% B in 0.1 min, isocratic for 5 min, decreasing to 5% B in 0.1 min, and re-equilibrating under the initial conditions for 5 min. Eluting compounds were detected by UV absorbance at 285 nm. **Method B.** Samples were separated on a Phenomenex Luna C18(2) column (4.6 mm × 250 mm, 5 μm) equilibrated with 70% solvent A (0.5% formic acid in H_2O) and 30% solvent B (0.5% formic acid in methanol) at a flow rate of 1 mL/min. The solvent was programmed as follows: a linear gradient from the starting solvent to 70% B in 20 min, increasing to 90% B in 0.1 min, isocratic for 5 min, decreasing to 30% B in 0.1 min, and re-equilibrating under the initial conditions for 5 min. Eluting compounds were detected by UV absorbance at 300 nm. **Method C.** Samples were separated on a Phenomenex Synergi POLAR-RP column (2.0 mm × 150 mm, 4 μm) equilibrated with 98% solvent A (0.5% formic acid in H_2O) and 2% solvent B (0.5% formic acid in methanol) at a flow rate of 0.3 mL/min. The solvent was programmed as follows: a linear gradient from the starting solvent to 40% B in 10 min, holding at 40% B for 3 min, decreasing to 2% B in 0.1 min, and holding under the initial conditions for 7 min. Eluting compounds were detected by UV absorbance at 254 and 275 nm. **Method D.** Samples were separated on a Phenomenex Luna C18(2) column (4.6 mm × 250 mm, 5 μm) equilibrated with 90% solvent A (0.5% formic acid in H_2O) and 10% solvent B (0.5% formic acid in methanol) at a flow rate of 1.0 mL/min. The solvent was programmed as follows: a linear gradient from the starting solvent to 20% B in 10 min, isocratic at 20% B for 10 min, increasing to 85% B in 0.1 min, isocratic at 85% B for 5 min, decreasing to 10% B in 0.1 min, and isocratic under the initial conditions for 5 min. Eluting compounds were detected by UV absorbance at 254 nm. **Method E.** Samples were separated on a Phenomenex Luna Phenyl-Hexyl column (4.6 mm × 250 mm, 5 μm) equilibrated with 90% solvent A [20 mM ammonium acetate (pH 7.0) in H_2O] and 10% solvent B [20 mM ammonium acetate (pH 7.0) in methanol] at a flow rate of 1.0 mL/min. The solvent was programmed as follows: a linear gradient from the starting solvent to 50% B in 10 min, decreasing to 10% B in 0.1 min, and isocratic under the initial conditions for 5 min. Eluting compounds were detected by UV absorbance at 254 and 285 nm.

Liver Cytosol Incubations. The following general incubation conditions were used for all substrates except where noted below. All sample preparation was performed on ice at 4 °C. Substrate stock solutions were dissolved in water. The final incubations contained 5 mg/mL rat liver cytosol, varied concentrations of substrates, 0.4% DMSO, and 0.1 M potassium phosphate (pH 7.4) buffer. All reagents were equilibrated to 37 °C for 5 min, and the reaction was initiated by the addition of substrate. Reactions were terminated by adding 0.5 mL of ice-cold ethanol, and the mixtures were vigorously mixed and extracted twice with 2 volumes of $CHCl_3$. The extracts were pooled, evaporated under nitrogen, and reconstituted in 0.1 M potassium phosphate (pH 7.4). All reactions were performed in triplicate. v_{max}/K_M and IC_{50} values were calculated with Prism (version 4.0c) using nonlinear regression one-site binding and one-site competition models, respectively.

1,N^2-ε-Gua and N^2,3-ε-Gua stock solutions were dissolved in 0.1 M NaOH; all incubations were conducted in 0.8 M potassium phosphate (pH 7.6), and extracted samples were dissolved in 0.1 M NaOH. 1,N^2-ε-Gua, 1,N^2-ε-dG, and N^2,3-ε-Gua were analyzed by chromatography method A. Heptanone-1,N^2-ε-dG and heptanone-1,N^2-ε-Gua stock solutions were dissolved in DMSO; all incuba-

tion preparation was performed at room temperature, and extracted samples were dissolved in methanol. Heptanone-1,N^2-ε-dG and heptanone-1,N^2-ε-Gua samples were analyzed by chromatography method B. 1,N^6-ε-dA incubations were also conducted in 0.1 M Tris-HCl buffer (pH 7.4). 1,N^6-ε-dA and 1,N^6-ε-Ade were analyzed by method C. 3,N^4-ε-dC, 3,N^4-ε-Cyt, 5,6-dihydro-M_1dG, 5,6-dihydro-M_1G, PdG, PGua, γ-OH-PdG, and α-OH-PdG reactions were terminated with ice-cold methanol, and the mixtures were vigorously mixed and centrifuged at 200000*g* for 30 min. Supernatants were removed and analyzed directly by chromatography method D, except for 3,N^4-ε-dC and 3,N^4-ε-Cyt, which were analyzed by method E.

Incubations of 1,N^2-ε-Gua with Purified XO. All sample preparation was performed on ice at 4 °C. The final incubations for the kinetic determinations contained 0.10 unit of XO/mL (CalBiochem), varied concentrations of 1,N^2-ε-Gua, and 0.4% DMSO in 0.8 M potassium phosphate (pH 7.6). Reagents were equilibrated to 37 °C for 5 min, and the reaction was initiated by the addition of the substrate. Reactions were terminated by adding 0.5 mL of ice-cold ethanol, and mixtures were vigorously mixed and extracted twice with 2 volumes of $CHCl_3$. The extracts were evaporated under nitrogen and reconstituted in 0.1 M NaOH. Samples were analyzed by chromatography method A. Samples from the kinetic determinations were quantified in reference to a standard curve prepared by spiking known concentrations of 1,N^2-ε-Gua into 0.10 unit/mL XO solutions, followed immediately by termination, extraction, and analysis as outlined above. All incubations and standards were performed in triplicate.

Incubations of 1,N^6-ε-dA and dIno with Purified Human PNP. All sample preparation was performed on ice at 4 °C. The specific activity of PNP was 18 units/mg. The final incubations for the kinetic determinations contained PNP (1.5 units/mL for 1,N^6-ε-Ade and 0.025 unit/mL for dIno reactions), varied concentrations of either 1,N^6-ε-Ade or dIno, and 0.8 M potassium phosphate (pH 7.6). Reagents were equilibrated to 37 °C for 5 min, and the reaction was initiated by the addition of substrate. Reactions were terminated with ice-cold ethanol, and mixtures were vigorously mixed, followed by the addition of 1 volume of $CHCl_3$. Samples were evaporated under nitrogen, reconstituted in 0.1 M potassium phosphate (pH 7.4), and analyzed by chromatography method C, with the flow rate adjusted to 1.0 mL/min. All incubations were prepared in triplicate.

LC−MS/MS Analysis. Following sample workup as noted above, selected samples were analyzed by LC−MS/MS analysis. The previously described chromatography methods (see above) were adapted to lower flow rates (0.3 mL/min) for sample analysis. Eluting compounds were analyzed on either ThermoElectron LTQ or Quantum instruments. Positive ion ESI LC−MS/MS or LC−MS^n was performed with the following general parameters: spray voltage, 4.2 eV; capillary temperature, 275 °C; sheath gas, 60 psi; source CID off; and varied collision energies.

Biochemical Synthesis of the 1,N^2-ε-Gua Metabolite [1H-imidazo[1,2-a]purine-2,9(3H,5H)-dione]. 1,N^2-ε-Gua (2 mg) was incubated with 5 mL of concentrated rat liver cytosol (13.6 mg/mL) and allowed to proceed to completion. The reaction mix was centrifuged at 10000*g* for 15 min to pellet protein, and the supernatant was injected directly onto the HPLC system. Fractions corresponding to the 1,N^2-ε-Gua metabolite were pooled, evaporated under reduced pressure, and dissolved in DMSO-d_6 for NMR analysis. Purified 2-oxo-ε-Gua was analyzed by HRMS to probe for the calculated *m/z* of $C_7H_6N_5O_2$ (M + H) of 191.1469 (found 191.0443).

Biochemical Synthesis of the Heptanone-1,N^2-ε-Gua Metabolite [7-(2-oxoheptyl)-1H-imidazo[1,2-a]purine-2,9(3H,5H)-dione]. Heptanone-1,N^2-ε-Gua (1 mg) was reacted in 30 mL of concentrated gerbil liver cytosol and allowed to proceed to completion. Fifteen milliliters of ethanol was added to the reaction mix and centrifuged at 10000*g* for 15 min to precipitate protein. An additional 15 mL of ethanol was added to the supernatant, and the mixture was extracted twice with 50 mL of chloroform. The organic layers were pooled and evaporated under reduced pressure. The remaining residue was redissolved in methanol and directly injected onto the HPLC system. Fractions corresponding to the heptanone-1,N^2-ε-Gua metabolite were collected, evaporated under reduced pressure, and dissolved in DMSO-d_6 for NMR analysis. Purified 2-oxoheptanone-ε-Gua was analyzed by HRMS to probe for the calculated *m/z* of $C_{14}H_{17}N_5O_3$ (M + H) of 303.3165 (found 303.1331).

NMR Analysis of 1,N^2-ε-Gua and Heptanone-1,N^2-ε-Gua Metabolites. NMR experiments were conducted using a 14.0 T Bruker magnet equipped with a Bruker AV-III console operating at 600.13 MHz. All spectra were acquired in 3 mm NMR tubes using a Bruker 5 mm TCI cryogenically cooled NMR probe. Chemical shifts were referenced internally to DMSO (0.49 ppm), which also served as the 2H lock solvent. For one-dimensional (1D) ^{1}H NMR, typical experimental conditions included 32K data points, a sweep width of 13 ppm, a recycle delay of 1.5 s, and 32−256 scans depending on sample concentration. For two-dimensional (2D) ^{1}H−^{1}H COSY, experimental conditions included 2048 × 512 data matrix, a sweep width of 13 ppm, a recycle delay of 1.5 s, and four scans per increment. The data were processed using a squared sine bell window function, symmetrized, and displayed in magnitude mode. Multiplicity-edited heteronuclear single-quantum coherence (HSQC) experiments were conducted using a 1024 × 256 data matrix, a *J*(C−H) value of 145 Hz which resulted in a multiplicity selection delay of 34 ms, a recycle delay of 1.5 s, and 16 scans per increment along with GARP decoupling on ^{13}C during the acquisition time (150 ms). The data were processed using a π/2 shifted squared sine window function and displayed with CH/CH_3 signals phased positive and CH_2 signals phased negative. J_1(C−H) filtered HMBC experiments were conducted using a 2048 × 256 data matrix, a *J*(C−H) value of 9 Hz for detection of long-range couplings resulting in an evolution delay of 55 ms, a J_1(C−H) filter delay of 145 Hz (34 ms) for the suppression of one-bond couplings, a recycle delay of 1.5 s, and 128 scans per increment. The HMBC data were processed using a π/2 shifted squared sine window function and displayed in magnitude mode.

RESULTS

Oxidation of 1,N^2-ε-Gua in Rat Liver Cytosol. 1,N^2-ε-Gua is released from DNA by the alkylpurine-DNA-*N*-glycosylase in mammalian cells (*25, 27*). The base adduct 1,N^2-ε-Gua is structurally very similar to the pyrimidopurinone adduct,

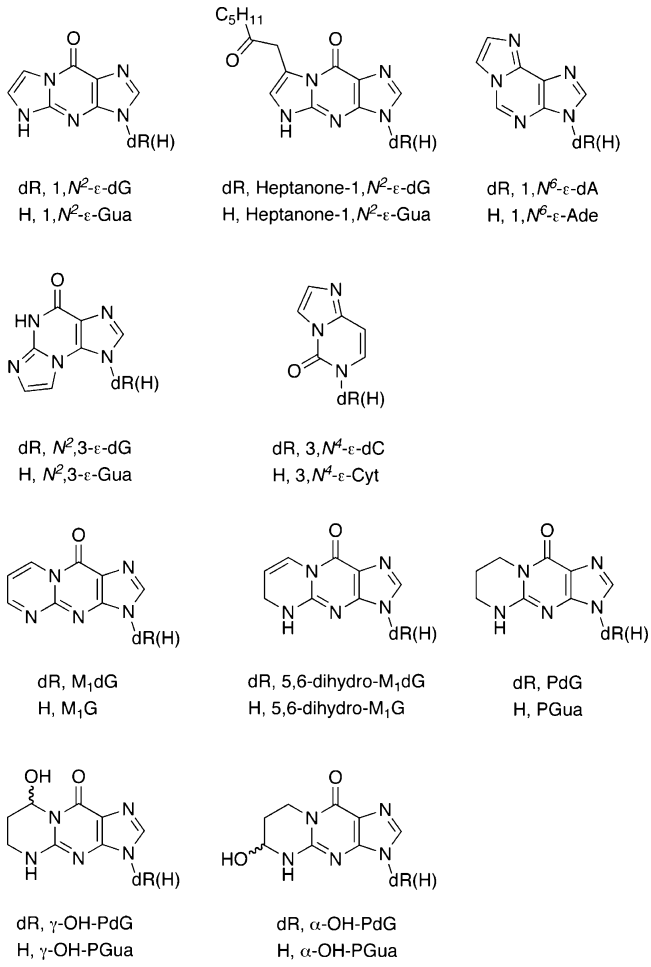

FIGURE 1: Structures of endogenously formed exocyclic DNA base adducts and structural analogues of M_1dG.

M_1G (Figure 1), which is a substrate for enzymatic oxidation in vitro and in vivo (*9*). To investigate whether 1,N^2-ε-Gua was also a substrate for oxidation, we performed in vitro experiments using rat liver cytosol. Profiling the reaction extracts by HPLC with UV detection demonstrated a time-dependent decrease in the level of N^2-ε-Gua and the appearance of a new peak eluting shortly after it. Positive ion ESI LC−MS analysis of the later eluting peak revealed an *m/z* of 192.1, which suggested the incorporation of a single oxygen atom. No additional products were observed in the MS or UV spectra. MS^n experiments were carried out on the putative metabolite, which displayed fragmentation patterns similar to those of 1,N^2-ε-Gua, except for the addition of 16 amu, which was apparent with the base peak and with some fragments (Figure 2). 1,N^2-ε-Gua metabolite production was inhibited by allopurinol, an inhibitor of xanthine oxidoreductase (XOR), but not by menadione or raloxifene, each an inhibitor of aldehyde oxidase (AO), which suggested the involvement of XOR in the oxidation of 1,N^2-ε-Gua (Figure 2).

Further investigation into the turnover of 1,N^2-ε-Gua in rat liver cytosol revealed a K_M of 84 μM and a v_{max} of 105 pmol min^{-1} mg^{-1} (v_{max}/K_M = 0.005 min^{-1} mg^{-1}) (Table 1). These calculated values are very close to what was observed for M_1G and 6-oxo-M_1G oxidation in rat liver cytosol (*9*). IC_{50} determinations with allopurinol on 1,N^2-ε-Gua oxidation revealed complete inhibition of metabolite production at saturating concentrations of allopurinol in rat liver cytosol (IC_{50} of 1.4 μM) (Figure 2).

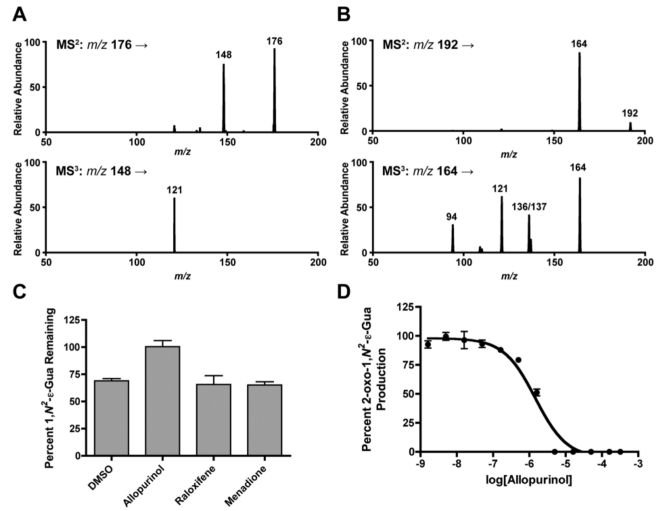

FIGURE 2: In vitro oxidation of 1,N^2-ε-Gua in rat liver cytosol. (A) MS^n fragmentation of 1,N^2-ε-Gua (*m/z* 176). (B) MS^n fragmentation of the 1,N^2-ε-Gua metabolite (*m/z* 192). (C) Effect of inhibitors of XOR (allopurinol) and AO (menadione and raloxifene) on the consumption of 1,N^2-ε-Gua in rat liver cytosol. (D) IC_{50} determination for the inhibition of the 1,N^2-ε-Gua metabolite in rat livery cytosol using 1,N^2-ε-Gua (84 μM) as a substrate. IC_{50} values were determined on the basis of 1,N^2-ε-Gua metabolite inhibition with increasing concentrations of allopurinol in rat liver cytosol (IC_{50} = 1.4 μM).

Table 1: K_m and v_{max} Values for the Oxidation of 1,N^2-ε-Gua, M_1G, 6-oxo-M_1G, and M_1dG in Rat Liver Cytosol

substrate	K_M (μM)	v_{max} (nmol min^{-1} mg^{-1})	v_{max}/K_M (min^{-1} mg^{-1})
1,N^2-ε-Gua	84	105	0.005
M_1G[a]	105	126	0.005
6-oxo-M_1G[a]	210	257	0.005
M_1dG[b]	370	104	0.001

[a] Values taken from ref *9*. [b] Values taken from ref *12*.

Oxidation of 1,N^2-ε-Gua with Purified XO. The complete inhibition of 1,N^2-ε-Gua oxidation by allopurinol suggested XOR was the only enzyme involved in the oxidation of 1,N^2-ε-Gua. In vitro oxidation of 1,N^2-ε-Gua was performed using purified bovine xanthine oxidase (XO). XO readily consumed 1,N^2-ε-Gua, demonstrating a K_M of 108 μM and a v_{max} of 10.1 μmol min^{-1} (mg of XO)$^{-1}$ (Figure 3).

Structural Characterization of the 1,N^2-ε-Gua Metabolite. To identify the product of 1,N^2-ε-Gua oxidation in rat liver cytosol, we biochemically synthesized the metabolite with concentrated rat liver cytosol and purified the product by fraction collection from a HPLC system. The product was concentrated and dissolved in DMSO-d_6 for NMR analysis. Comparison of the ^{1}H NMR spectra for 1,N^2-ε-Gua and the metabolite revealed an absence of the singlet corresponding to H2 (7.8 ppm) from the imidazole ring, while two correlated doublets remained from the etheno ring for H7 (d, 1H, 7.6 ppm) and H6 (d, 1H, 7.4 ppm) (Figure 4) (*37*). This was confirmed by the HSQC spectrum, which demonstrated the metabolite contained only CH protons (Figure S1 of the Supporting Information). If oxidation had occurred on the etheno ring, the carbon adjacent to the site of oxidation would have been reduced to CH_2. HMBC analysis revealed three-bond couplings for H7 and H6 to C4a (145 ppm),

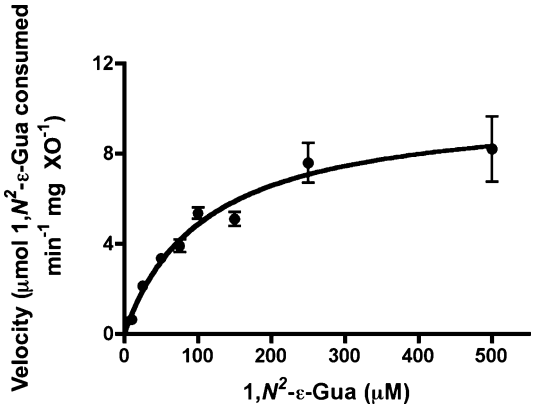

FIGURE 3: Concentration dependence of 1,N^2-ε-Gua oxidation in purified XOR. 1,N^2-ε-Gua consumption was assessed using XOR purified from bovine milk. Kinetic determinations were made in reference to a standard curve for the consumption of 1,N^2-ε-Gua [K_M = 108 μM, and v_{max} = 10.1 μmol min^{-1} (mg of XOR)$^{-1}$].

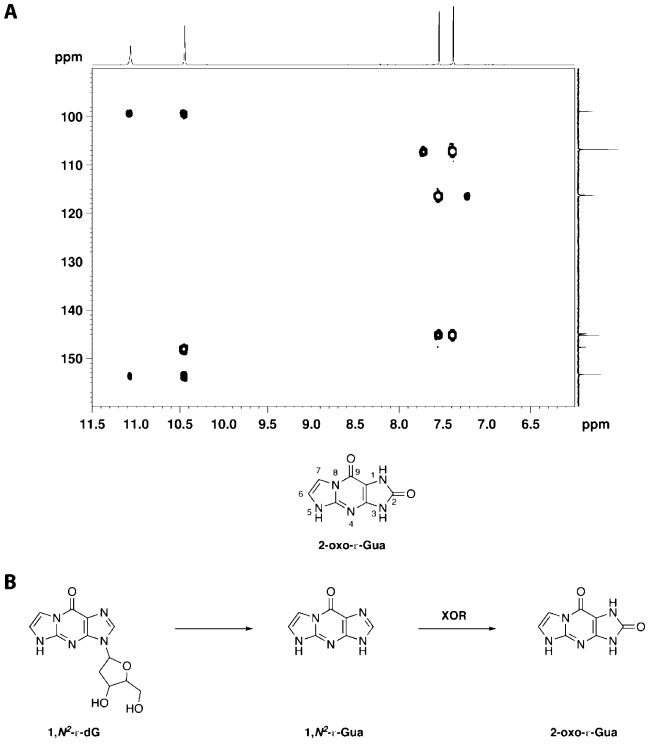

FIGURE 4: Structural determination of the 1,N^2-ε-Gua metabolite as 2-oxo-1,N^2-ε-Gua. (A) HMBC spectrum of the 1,N^2-ε-Gua metabolite from rat liver cytosol confirming the structure as 2-oxo-ε-Gua. (B) 1,N^2-ε-dG undergoes glycolytic cleavage to 1,N^2-ε-Gua in rat liver cytosol, which is then oxidized by XOR to 2-oxo-ε-Gua.

confirming oxidation had not occurred on the etheno ring, but on the imidazole ring yielding 2-oxo-ε-Gua (Figure 4).

Glycolytic Cleavage of 1,N^2-ε-dG in Rat Liver Cytosol. The observed oxidation of 1,N^2-ε-Gua in rat liver cytosol led us to investigate the stability of the 2′-deoxynucleoside, 1,N^2-ε-dG. We were curious to know if oxidation would occur on the imidazole ring of the etheno adduct containing 2′-deoxyribose. Incubation conditions identical to those of 1,N^2-ε-Gua studies were used with 1,N^2-ε-dG in rat liver cytosol. The 2′-deoxynucleoside adduct did not undergo oxidation. However, LC−UV and LC−MS analysis of the reaction mixture indicated 1,N^2-ε-dG was consumed over time, producing a new chromatographic peak eluting with an identical retention time and mass spectrum for the base, 1,N^2-ε-Gua. Furthermore, the newly produced 1,N^2-ε-Gua was converted to the oxidized product, 2-oxo-ε-Gua. There was no evidence to support direct oxidation of the 2′-deoxynucleoside. These data suggested 1,N^2-ε-dG was subject to glycolytic cleavage in rat liver cytosol, and the product of this conversion was subsequently oxidized (Figure 4).

Glycolytic cleavage was not observed with M_1dG either in vitro in rat liver cytosol or in vivo in the rat (*11, 12*). Results with 1,N^2-ε-dG suggest the involvement of an additional pathway for exocyclic adduct biotransformation. Purine nucleoside phosphorylase (PNP) is an enzyme involved in purine catabolism as part of the purine salvage pathway. PNP carries out the glycolytic cleavage of 6-oxopurine nucleosides and 2′-deoxynucleosides [guanosine, inosine, dG, and 2′-deoxyinosine (dIno)] to their corresponding bases (Gua and hypoxanthine). The enzyme uses inorganic phosphate ($H_2PO_4^-$) as a cosubstrate and produces (2′-deoxy)ribose-1-phosphate in addition to the base. PNP is expressed in rat liver (*38, 39*). The observed cleavage of 1,N^2-ε-dG to 1,N^2-ε-Gua suggests the involvement of PNP in rat liver cytosol.

Oxidation of Heptanone-1,N^2-ε-Gua in Rat Liver Cytosol. Two exocyclic base adducts (6-oxo-M_1G and 1,N^2-ε-Gua) undergo enzymatic oxidation on the imidazole ring. In both instances, the presence of the 2′-deoxyribose moiety on the imidazole portion of the base retards this oxidation. As a corollary, we were curious to know what effects etheno ring substituents would have on imidazole oxidation. To address this question, we investigated the endogenously produced heptanone-1,N^2-ε-dG, which contains a 2-oxoheptyl side chain extending off of C7 on the etheno ring (Figure 1) (*33*). We performed in vitro experiments using rat liver cytosol with heptanone-1,N^2-ε-dG and its corresponding base, heptanone-1,N^2-ε-Gua. The 2′-deoxynucleoside was stable in rat liver cytosol and was a substrate for neither oxidation nor glycolytic cleavage. However, the base adduct heptanone-1,N^2-ε-Gua was oxidized. Profiling the reaction mixtures by LC−MS/MS revealed a new peak eluting shortly after heptanone-1,N^2-ε-Gua. MS^n experiments were conducted with the putative heptanone-1,N^2-ε-Gua metabolite, which displayed fragmentation patterns similar to those of heptanone-1,N^2-ε-Gua, except for the addition of 16 amu, which was apparent with the base peak and with some fragments (Figure 5). The use of chemical inhibitors suggested the involvement of XOR because co-incubation with allopurinol inhibited oxidation, but co-incubation with either menadione or raloxifene did not (Figure 5). Limitations in analyte solubility precluded concentration-dependent kinetic determinations in rat liver cytosol.

Biochemical Synthesis of the Heptanone-1,N^2-ε-Gua Metabolite. Heptanone-1,N^2-ε-Gua was reacted to completion in concentrated gerbil liver cytosol, extracted, and purified by reverse phase HPLC. HPLC fractions containing the metabolite were concentrated and dissolved in DMSO-d_6 for analysis by NMR. The HSQC and HMBC experiments enabled identification of the metabolite as 2-oxoheptanone-ε-Gua (Figure 6). H6 (s, 1H, 7.1 ppm, C6 at 116 ppm) was evident in the HSQC spectrum and showed a two-bond correlation to C7 (119 ppm) and a three-bond correlation to C4a (146 ppm) in the HMBC spectrum. H1′ (s, 2H, 4.1 ppm,

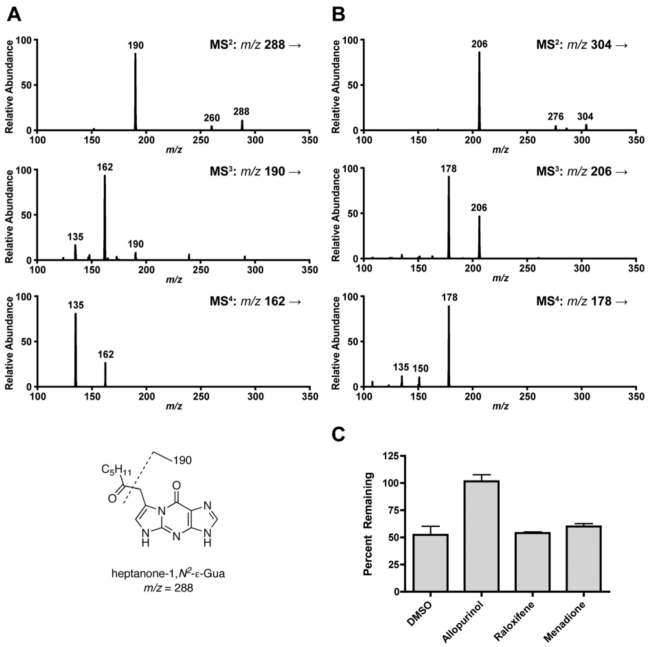

FIGURE 5: In vitro oxidation of heptanone-1,N^2-ε-Gua in rat liver cytosol. (A) MS^n fragmentation of heptanone-1,N^2-ε-Gua (*m*/*z* 288). (B) MS^n fragmentation of the heptanone-1,N^2-ε-Gua metabolite (*m*/*z* 304). (C) Effect of inhibitors of XOR (allopurinol) and AO (menadione and raloxifene) on the consumption of heptanone-1,N^2-ε-Gua in rat liver cytosol.

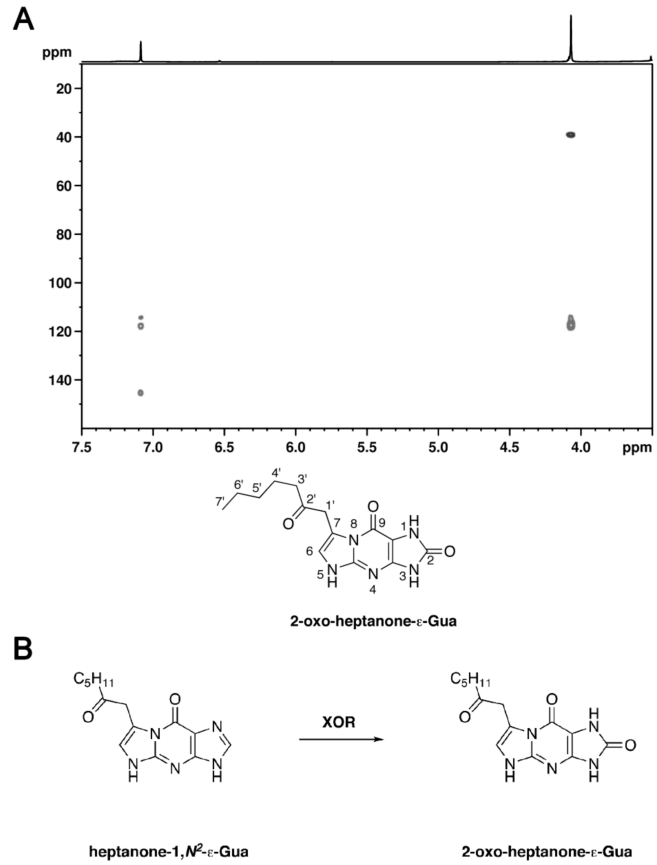

FIGURE 6: Structural determination of the heptanone-1,N^2-ε-Gua metabolite as 2-oxoheptanone-1,N^2-ε-Gua. (A) Overlay of the HSQC and HMBC spectra for the biochemically synthesized heptanone-1,N^2-ε-Gua metabolite, which confirmed the structure as 2-oxoheptanone-ε-Gua. (B) Heptanone-1,N^2-ε-Gua is oxidized to 2-oxoheptanone-ε-Gua in liver cytosol by XOR.

C1′ at 39 ppm) was evident in the HSQC spectrum and exhibited two-bond correlations to C7 (119 ppm) and C2′ (206 ppm) and a three-bond coupling to C6 (116 ppm) in the HMBC spectrum. The three-bond coupling from H6 to C1′ was not observed, however. Direct comparison of the metabolite spectra to the heptanone-1,N^2-ε-Gua spectra was inconclusive. Several additional chemical shifts were observed in the starting material, which were an artifact of the sample workup, and attributed to the equilibrium between heptanone-1,N^2-ε-Gua and the hemiketal (*33*).

Investigation of N^2,3-ε-Gua, 3,N^4-ε-dC, 3,N^4-ε-Cyt, 1,N^6-ε-dA, and 1,N^6-ε-Ade Stability. Several exocyclic adducts of dG have been characterized as undergoing oxidation in rat liver cytosol. The 1,N^2-ε-Gua isomer, N^2,3-ε-Gua, is derived from lipid peroxidation and is a substrate for repair by DNA glycosylase (*24, 40*). The exocyclic etheno ring of N^2,3-ε-Gua is positioned more proximal to the imidazole ring of guanine and represents a greater departure from the M_1G template. Incubation of N^2,3-ε-Gua in either rat liver cytosol or purified bovine XO did not result in oxidative metabolism; thus, the adduct was stable to enzymatic oxidation.

3,N^4-ε-dC and 1,N^6-ε-dA are etheno adducts of dC and dA (Figure 1), respectively, with proposed routes of endogenous formation (*41, 42*). 3,N^4-ε-dC and 1,N^6-ε-dA are released from DNA by glycosylase action as the corresponding base adducts, 3,N^4-ε-Cyt (*26, 28*) and 1,N^6-ε-Ade (*25, 28*), respectively. The exocyclic etheno rings for these molecules are structurally similar and contain a heterocyclic imine extending from a quaternary carbon on the base, which is a pyrimidine in the case of 3,N^4-ε-Cyt and purine for 1,N^6-ε-Ade. Each base adduct was investigated for enzymatic oxidation in rat liver cytosol, but neither was found to be oxidized.

The corresponding 2′-deoxynucleoside adducts 3,N^4-ε-dC and 1,N^6-ε-dA were also investigated for their stability in rat liver cytosol. The reaction mixtures were profiled by positive ion ESI LC−MS/MS, and neither of these adducts was found to be oxidized in vitro. However, 1,N^6-ε-dA underwent a time-dependent decrease in total peak area, with a corresponding increase of an early eluting peak, which displayed an ion at *m*/*z* 162.1. The appearance of the ion at *m*/*z* 162.1 was not detected in control incubations. The early eluting peak corresponded to the protonated molecular ion for the base (1,N^6-ε-Ade), suggesting that 1,N^6-ε-dA underwent glycolytic cleavage. This product also cochromatographed when the incubation extract was spiked with an authentic 1,N^6-ε-Ade standard. Identical observations were made using 1,N^6-ε-adenosine in incubations with rat liver cytosol.

To investigate the role of PNP, which uses $H_2PO_4^-$ as a cosubstrate in the glycolytic cleavage of 1,N^6-ε-dA, we performed rat liver cytosol incubations using either potassium phosphate or Tris-HCl buffers. In the absence of inorganic phosphate, the production of 1,N^6-ε-Ade was diminished (Figure 7). 1,N^6-ε-dA was also incubated in reactions with purified PNP from human blood using potassium phosphate buffer. Glycolytic cleavage of 1,N^6-ε-dA was dependent on protein concentration and incubation time. Determinations of v_{max}/K_M for 1,N^6-ε-dA turnover in purified PNP were extrapolated from the linear portion of the *v* versus *S* plot. Turnover of dIno (a natural substrate for PNP) under similar reaction conditions revealed that the efficiency of turnover

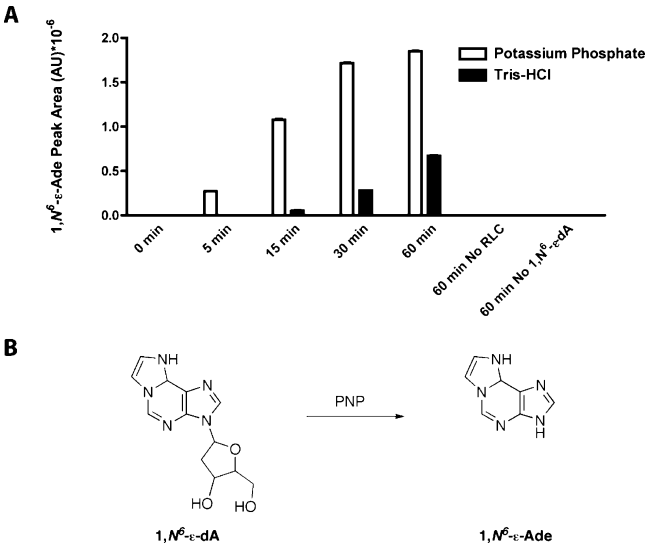

FIGURE 7: Conversion of 1,N^6-ε-dA to 1,N^6-ε-Ade in rat liver cytosol. (A) Effect of either potassium phosphate or Tris-HCl buffer on the conversion of 1,N^6-ε-dA (100 μM) to 1,N^6-ε-Ade in rat liver cytosol. (B) Conversion of 1,N^6-ε-dA to 1,N^6-ε-Ade carried out by PNP.

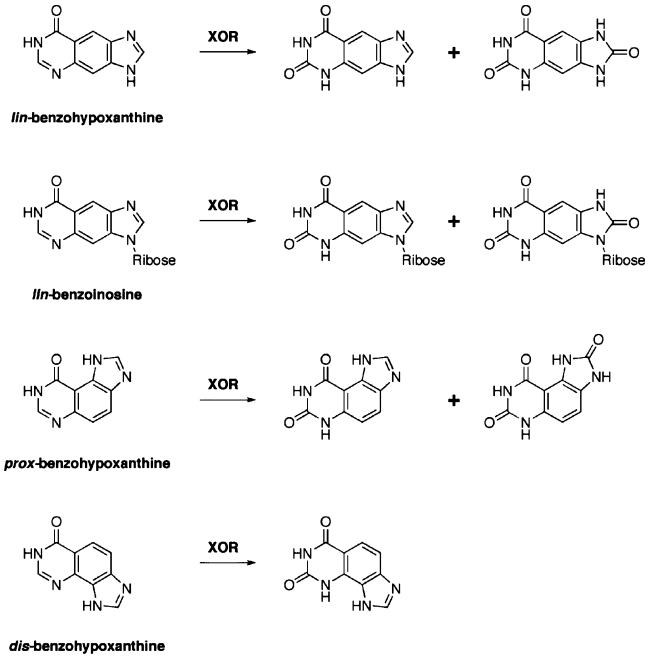

FIGURE 8: Structures of stretched-out 6-oxopurine analogues synthesized by Leonard et al. (*51*) and their conversion to oxidized products by XO from bovine milk.

for dIno (16.6 min^{-1}) was approximately 57-fold greater than that for 1,N^6-ε-dA (0.3 min^{-1}).

Investigation of M_1dG Analogues in Rat Liver Cytosol. To lend further insight into the structural requirements for the oxidation and glycolytic cleavage of exocyclic adducts in rat liver cytosol, we investigated the stability of several pyrimidopurinone−dG analogues of M_1dG and M_1G (Figure 1). The partially reduced pyrimido analogues 5,6-dihydro-M_1dG and 5,6-dihydro-M_1G and fully reduced analogues PdG and PGua have previously been used to mimic the biological activity of M_1dG in several genetic and biochemical investigations (*22, 30*). γ-OH-PdG and α-OH-PdG are endogenous adducts produced from reactions of acrolein with dG (*43*). These dG modifications impart different electronic and structural features on the exocyclic ring. For example, the pyrimido ring is planar and aromatic, whereas the propano ring is puckered and unconjugated. Members of this series of dG adducts are approximately the same size as the pyrimidopurinone adducts, so the exocyclic propano ring should not preclude access to the active sites of XOR, AO, or PNP. All investigations in rat liver cytosol with the 2′-deoxynucleoside structural analogues revealed no indication of either oxidation or glycolytic cleavage. Additionally, none of the base adducts was oxidized.

DISCUSSION

Non-invasive analysis of endogenously occurring DNA damage is of interest for use in clinical and animal studies. We propose that it is important to consider the possibility of biological processing during the development of analytical methods designed to evaluate endogenous levels of adducts. Although the elimination of DNA adducts in the urine is typically attributed to repair-dependent removal from DNA, it is important to consider that multiple factors may contribute to or limit their steady-state elimination rates (*7, 44, 45*). The contribution of modified DNA bases in the nucleotide pool, the release of adducts from apoptotic and necrotic cells, and the introduction of lesions from dietary intake may contribute to the levels of DNA base adducts in biological matrixes. However, these sources have not been fully evaluated. Additionally, the biliary elimination of adducts into the feces reduces the amount of adducts available for detection from urine samples (*10*). Independent of the route of formation in vivo, the metabolic processing of adducts as they pass through the circulatory system may limit their direct detection in biological matrixes.

This study was designed to determine structural features of exocyclic adducts that leads to oxidation. We focused our investigation on small changes in the pyrimido ring of M_1dG that imparted alterations to size and conjugation as well as the addition of substituents. In total, our findings demonstrate that the enzymatic oxidation of DNA base adducts can occur either on the exocyclic ring, as seen with M_1dG and M_1G, or on the imidazole ring, as seen with 6-oxo-M_1G, 1,N^2-ε-Gua, and heptanone-1,N^2-ε-Gua. Both 2′-deoxynucleosides and bases are subject to oxidation, with the base adducts being better substrates. When attached to the base, 2′-deoxyribose appears to prohibit oxidation on the imidazole ring. Additionally, biological processing is not limited to oxidation, as 2′-deoxynucleosides and nucleosides may also undergo glycolytic cleavage to the corresponding base adducts. We did not observe oxidation with dA, Ade, dC, or Cyt etheno adducts, but this does not preclude others derivatives of dA, Ade, dC, or Cyt from biotransformation.

The absence of oxidative metabolism for 1,N^6-ε-Ade and 3,N^4-ε-Cyt is noteworthy since both adducts have been implicated as substrates for oxidative DNA repair. The DNA repair enzyme AlkB utilizes non-heme iron, oxygen, and α-ketoglutarate to repair alkyl DNA damage; the human ortholog, hABH2, likely acts by a similar mechanism (*46, 47*). AlkB oxidizes both 1,N^6-ε-Ade and 3,N^4-ε-Cyt to generate epoxide and glyoxal intermediates prior to complete removal of the etheno bridge. This oxidative mechanism is a departure from the oxidation carried out by AO and XOR, which incorporate water (not molecular oxygen) from the molybdopterin active site (*48*).

There are multiple reports on the structural determinants of XOR and AO substrate specificity and inhibition (*49–54*). In general, substrates are nitrogen-containing heterocycles, and the enzyme-mediated oxidation is targeted to electropositive carbons, which lie adjacent to ring nitrogens (*54*). Our observations with exocyclic adducts are consistent with these observations.

In a series of biochemical experiments, Leonard et al. (*51, 52*) demonstrated XOR-mediated oxidation with several modified purine structures that are structurally similar to the pyrimido and etheno adducts of dG (Gua) and dA (Ade) (Figure 8). Inserting a benzene ring between the imidazole and pyrimidine rings of 6-oxopurine (hypoxanthine) yielded several "stretched-out" purine analogues. *lin*-Benzohypoxanthine is similar to M_1G; however, for M_1G, the benzene ring is attached to the pyrimidine opposite the imidazole ring, not beween the pyrimidine and imidazole ring. Using bovine XOR, Leonard et al. demonstrated successive oxidations of *lin*-benzohypoxanthine to uric acid-like molecules. This is analogous to what was previously observed with M_1G (*9*). Interestingly, Leonard et al. also observed successive oxidations with the ribonucleoside, *lin*-benzoinosine. In our investigations, oxidation on the imidazole ring did not occur with any 2′-deoxynucleoside-containing base adducts.

Thus far, all characterized oxidation products of exocyclic adducts occur on imine carbons of either the exocyclic or imidazole rings. Reduction of the 5,6-double bond on the pyrimido ring of M_1dG (M_1G) yields a saturated carbon at the 6-position, and fully reducing the exocyclic ring produces a fully saturated propano ring. Neither of these analogues of M_1dG (M_1G) underwent oxidation in rat liver cytosol. Krenitsky et al. demonstrated that purine is oxidized by XOR first at the 6-position and then successively at the 2- and 8-positions. However, AO oxidizes purine only at the 8-posititon on the imidazole carbon (*49*). The analogous position on the M_1G analogues is the 2-position, which was not a target for oxidation by AO or XOR. However, the imidazole ring of 1,N^2-ε-Gua was targeted for oxidation by XOR. The exocyclic ring of 1,N^2-ε-Gua is only one carbon larger than M_1G. This would imply that the XOR active site cannot accommodate this small increase, and this cannot be overcome by reducing the nonplanar character of the pyrimido ring.

The effect of substitutions on the exocyclic ring of propano and etheno dG adducts was investigated. PdG adducts with hydroxyl substituents on the exocyclic ring did not undergo biological processing, although the base adducts were not investigated. The addition of an alkyl substituent on the exocyclic ring of heptanone-1,N^2-ε-Gua did influence oxidation, however. Heptanone-1,N^2-ε-Gua underwent oxidation at the 2-position of the imidazole ring, whereas the 2′-deoxynucleoside was not modified. Heptanone-1,N^2-ε-dG did not undergo glycolytic cleavage as seen with the unsubstituted 1,N^2-ε-dG. Several recent reports from Blair and colleagues suggest substituted etheno adducts of dA, dC, and dG comprise a major class of endogenous adducts derived from products of lipid peroxidation (*4, 33, 55–58*). The repair products of these unsubstituted adducts are unknown; therefore, the biological processing of heptanone-1,N^2-ε-Gua may be of interest when monitoring its levels from biological matrixes. Additionally, several purine-based therapeutics (aciclovir, penciclovir, and zaleplon) and other substituted purine molecules are substrates for oxidation by AO and XOR (*49, 59, 60*). Thus, it will be interesting to elucidate the biochemical processing of other substituted etheno adducts.

PNP is a central enzyme in the purine salvage pathway. The enzyme functions to both synthesize and cleave nucleosides and 2′-deoxynucleosides, but the cleavage reaction (phosphorolysis) is generally favored in vivo. In general, substrates for the mammalian enzyme are 6-oxopurines and their corresponding nucleosides and 2′-deoxynucleosides, although PNP is typically less active toward 6-aminopurines. Our observation of 1,N^6-ε-dA, which lacks the 6-oxo group, as a moderate substrate for phosphorolysis is of interest. Modification of adenosine nucleosides with alkyl substituents on the purine ring has previously been shown to increase the rate of phosphorolysis (*39*).

1,N^2-ε-dG and 1,N^6-ε-dA underwent glycolytic cleavage to base adducts 1,N^2-ε-Gua and 1,N^6-ε-Ade, respectively, in rat liver cytosol. Both of these base adducts have been detected in urine from humans and rats (*8, 61*). The elimination of these adducts in urine has generally been attributed to their removal from DNA as base adducts. Interestingly, 1,N^6-ε-dA has also been detected in rat urine (*7*). On the basis of our results, 1,N^6-ε-Ade may be the best target for quantification in urine samples. This hypothesis is also supported by a previous in vivo study on the metabolism and elimination of ^{14}C-labeled 1,N^6-ε-adenosine (*62*), which suggested a significant percentage of exogenously administered 1,N^6-ε-adenosine was eliminated in urine as the free base, 1,N^6-ε-Ade.

Since endogenously formed exocyclic adducts are all modifications of purine and pyrimidine structures, we targeted our investigation to the cytosolic components of rat liver where XOR and AO are located. It is possible that other enzymes may catalyze the biotransformation of exocyclic adducts. CYPs and UDP-glucuronosyl transferases (components of the microsomal fraction of rat liver) may have a role in biotransformation. Our results with the propano analogues suggest they are stable in vitro in rat liver cytosol. Propano adducts derived from crotonaldehyde and 4-hydroxy-2-nonenal also have alkyl substituents extended from the exocyclic ring, which may be targeted by different enzymes and alternate routes of biological processing.

Understanding the in vitro routes of biological processing should help guide the development of analytical methodologies for the detection of endogenous adducts. Several exocyclic adducts have been characterized as good substrates for oxidation in vitro. The end products of biological processing may therefore be reliable targets for assessing the formation of endogenous adducts from biological matrixes in vivo.

SUPPORTING INFORMATION AVAILABLE

HSQC spectrum for the 2-oxo-ε-Gua metabolite. This material is available free of charge via the Internet at http://pubs.acs.org.

REFERENCES

1. Klaunig, J. E., and Kamendulis, L. M. (2004) The role of oxidative stress in carcinogenesis. *Annu. Rev. Pharmacol. Toxicol. 44*, 239–267.

2. Dedon, P. C., and Tannenbaum, S. R. (2004) Reactive nitrogen species in the chemical biology of inflammation. *Arch. Biochem. Biophys. 423*, 12–22.
3. Meira, L. B., Bugni, J. M., Green, S. L., Lee, C. W., Pang, B., Borenshtein, D., Rickman, B. H., Rogers, A. B., Moroski-Erkul, C. A., McFaline, J. L., Schauer, D. B., Dedon, P. C., Fox, J. G., and Samson, L. D. (2008) DNA damage induced by chronic inflammation contributes to colon carcinogenesis in mice. *J. Clin. Invest. 118*, 2516–2525.
4. Williams, M. V., Lee, S. H., Pollack, M., and Blair, I. A. (2006) Endogenous lipid hydroperoxide-mediated DNA-adduct formation in min mice. *J. Biol. Chem. 281*, 10127–10133.
5. World Health Organization (2001) *IPCS Environmental Health Criteria 222: Biomarkers and Risk Assessment: Validity and Validation*, World Health Organization, Geneva.
6. Sharma, R. A., and Farmer, P. B. (2004) Biological relevance of adduct detection to the chemoprevention of cancer. *Clin. Cancer Res. 10*, 4901–4912.
7. Yen, T. Y., Holt, S., Sangaiah, R., Gold, A., and Swenberg, J. A. (1998) Quantitation of 1,N^6-ethenoadenine in rat urine by immunoaffinity extraction combined with liquid chromatography/electrospray ionization mass spectrometry. *Chem. Res. Toxicol. 11*, 810–815.
8. Chen, H. J., and Chiu, W. L. (2005) Association between cigarette smoking and urinary excretion of 1,N^2-ethenoguanine measured by isotope dilution liquid chromatography-electrospray ionization/tandem mass spectrometry. *Chem. Res. Toxicol. 18*, 1593–1599.
9. Knutson, C. G., Akingbade, D., Crews, B. C., Voehler, M., Stec, D. F., and Marnett, L. J. (2007) Metabolism *in vitro* and *in vivo* of the DNA base adduct, M_1G. *Chem. Res. Toxicol. 20*, 550–557.
10. Knutson, C. G., Skipper, P. L., Liberman, R. G., Tannenbaum, S. R., and Marnett, L. J. (2008) Monitoring in vivo metabolism and elimination of the endogenous DNA adduct, M_1dG {3-(2-deoxy-β-D-*erythro*-pentofuranosyl)pyrimido[1,2-α]purin-10(3*H*)-one}, by accelerator mass spectrometry. *Chem. Res. Toxicol. 21*, 1290–1294.
11. Knutson, C. G., Wang, H., Rizzo, C. J., and Marnett, L. J. (2007) Metabolism and elimination of the endogenous DNA adduct, 3-(2-deoxy-β-D-erythropentofuranosyl)-pyrimido[1,2-α]purine-10(3*H*)-one, in the rat. *J. Biol. Chem. 282*, 36257–36264.
12. Otteneder, M. B., Knutson, C. G., Daniels, J. S., Hashim, M., Crews, B. C., Remmel, R. P., Wang, H., Rizzo, C., and Marnett, L. J. (2006) In vivo oxidative metabolism of a major peroxidation-derived DNA adduct, M_1dG. *Proc. Natl. Acad. Sci. U.S.A. 103*, 6665–6669.
13. Diczfalusy, U., Falardeau, P., and Hammarstrom, S. (1977) Conversion of prostaglandin endoperoxides to C17-hydroxy acids catalyzed by human platelet thromboxane synthase. *FEBS Lett. 84*, 271–274.
14. Hamberg, M., and Samuelsson, B. (1967) Oxygenation of unsaturated fatty acids by the vesicular gland of sheep. *J. Biol. Chem. 242*, 5344–5354.
15. Basu, A. K., O'Hara, S. M., Valladier, P., Stone, K., Mols, O., and Marnett, L. J. (1988) Identification of adducts formed by reaction of guanine nucleosides with malondialdehyde and structurally related aldehydes. *Chem. Res. Toxicol. 1*, 53–59.
16. Seto, H., Okuda, T., Takesue, T., and Ikemura, T. (1983) Reaction of malondialdehyde with nucleic acid. I. Formation of fluorescent pyrimido[1,2-α]purin-10(3H)-one nucleosides. *Bull. Chem. Soc. Jpn. 56*, 1799–1802.
17. Dedon, P. C., Plastaras, J. P., Rouzer, C. A., and Marnett, L. J. (1998) Indirect mutagenesis by oxidative DNA damage: Formation of the pyrimidopurinone adduct of deoxyguanosine by base propenal. *Proc. Natl. Acad. Sci. U.S.A. 95*, 11113–11116.
18. Zhou, X., Taghizadeh, K., and Dedon, P. C. (2005) Chemical and biological evidence for base propenals as the major source of the endogenous M_1dG adduct in cellular DNA. *J. Biol. Chem. 280*, 25377–25382.
19. Jeong, Y. C., and Swenberg, J. A. (2005) Formation of M_1G-dR from endogenous and exogenous ROS-inducing chemicals. *Free Radical Biol. Med. 39*, 1021–1029.
20. Fink, S. P., Reddy, G. R., and Marnett, L. J. (1997) Mutagenicity in *Escherichia coli* of the major DNA adduct derived from the endogenous mutagen malondialdehyde. *Proc. Natl. Acad. Sci. U.S.A. 94*, 8652–8657.
21. VanderVeen, L. A., Hashim, M. F., Shyr, Y., and Marnett, L. J. (2003) Induction of frameshift and base pair substitution mutations by the major DNA adduct of the endogenous carcinogen malondialdehyde. *Proc. Natl. Acad. Sci. U.S.A. 100*, 14247–14252.
22. Johnson, K. A., Fink, S. P., and Marnett, L. J. (1997) Repair of propanodeoxyguanosine by nucleotide excision repair in vivo and in vitro. *J. Biol. Chem. 272*, 11434–11438.
23. Hoberg, A. M., Otteneder, M., Marnett, L. J., and Poulsen, H. E. (2004) Measurement of the malondialdehyde-2′-deoxyguanosine adduct in human urine by immuno-extraction and liquid chromatography/atmospheric pressure chemical ionization tandem mass spectrometry. *J. Mass Spectrom. 39*, 38–42.
24. Dosanjh, M. K., Chenna, A., Kim, E., Fraenkelconrat, H., Samson, L., and Singer, B. (1994) All 4 known cyclic adducts formed in DNA by the vinyl-chloride metabolite chloroacetaldehyde are released by a human DNA glycosylase. *Proc. Natl. Acad. Sci. U.S.A. 91*, 1024–1028.
25. Singer, B., Antoccia, A., Basu, A. K., Dosanjh, M. K., Fraenkel-Conrat, H., Gallagher, P. E., Kusmierek, J. T., Qiu, Z. H., and Rydberg, B. (1992) Both purified human 1,N^6-ethenoadenine-binding protein and purified human 3-methyladenine-DNA glycosylase act on 1,N^6-ethenoadenine and 3-methyladenine. *Proc. Natl. Acad. Sci. U.S.A. 89*, 9386–9390.
26. Hang, B., Medina, M., Fraenkel-Conrat, H., and Singer, B. (1998) A 55-kDa protein isolated from human cells shows DNA glycosylase activity toward 3,N^4-ethenocytosine and the G/T mismatch. *Proc. Natl. Acad. Sci. U.S.A. 95*, 13561–13566.
27. Saparbaev, M., Langouet, S., Privezentzev, C. V., Guengerich, F. P., Cai, H., Elder, R. H., and Laval, J. (2002) 1,N^2-Ethenoguanine, a mutagenic DNA adduct, is a primary substrate of *Escherichia coli* mismatch-specific uracil-DNA glycosylase and human alkylpurine-DNA-N-glycosylase. *J. Biol. Chem. 277*, 26987–26993.
28. Saparbaev, M., and Laval, J. (1998) 3,N^4-Ethenocytosine, a highly mutagenic adduct, is a primary substrate for *Escherichia coli* double-stranded uracil-DNA glycosylase and human mismatch-specific thymine-DNA glycosylase. *Proc. Natl. Acad. Sci. U.S.A. 95*, 8508–8513.
29. Szekely, J., Wang, H., Peplowski, K. M., Knutson, C. G., Marnett, L. J., and Rizzo, C. J. (2008) "One-pot" syntheses of malondialdehyde adducts of nucleosides. *Nucleosides, Nucleotides Nucleic Acids 27*, 103–109.
30. VanderVeen, L. A., Druckova, A., Riggins, J. N., Sorrells, J. L., Guengerich, F. P., and Marnett, L. J. (2005) Differential DNA recognition and cleavage by EcoRI dependent on the dynamic equilibrium between the two forms of the malondialdehyde-deoxyguanosine adduct. *Biochemistry 44*, 5024–5033.
31. Marinelli, E. R., Johnson, F., Iden, C. R., and Yu, P. L. (1990) Synthesis of 1,N^2-(1,3-propano)-2′-deoxyguanosine and incorporation into oligodeoxynucleotides: A model for exocyclic acrolein-DNA adducts. *Chem. Res. Toxicol. 3*, 49–58.
32. Sattsangi, P. D., Leonard, N. J., and Frihart, C. R. (1977) 1,N^2-Ethenoguanine and N^2,3-ethenoguanine. Synthesis and comparison of the electronic spectral properties of these linear and angular triheterocycles related to the Y bases. *J. Org. Chem. 42*, 3292–3296.
33. Rindgen, D., Nakajima, M., Wehrli, S., Xu, K., and Blair, I. A. (1999) Covalent modifications to 2′-deoxyguanosine by 4-oxo-2-nonenal, a novel product of lipid peroxidation. *Chem. Res. Toxicol. 12*, 1195–1204.
34. Secrist, J. A., III., Barrio, J. R., Leonard, N. J., and Weber, G. (1972) Fluorescent modification of adenosine-containing coenzymes. Biological activities and spectroscopic properties. *Biochemistry 11*, 3499–3506.
35. Barrio, J. R., Secrist, J. A., III., and Leonard, N. J. (1972) Fluorescent adenosine and cytidine derivatives. *Biochem. Biophys. Res. Commun. 46*, 597–604.
36. Guengerich, F. P. (1994) Analysis and Characterization of Enzymes. In *Principles and Methods of Toxicology* (Hayes, A. W., Ed.) 3rd ed., pp 1259−1313, Raven Press Ltd., New York.
37. Guengerich, F. P., Persmark, M., and Humphreys, W. G. (1993) Formation of 1,N^2- and N^2,3-ethenoguanine from 2-halooxiranes: Isotopic labeling studies and isolation of a hemiaminal derivative of N^2-(2-oxoethyl)guanine. *Chem. Res. Toxicol. 6*, 635–648.
38. Friedkin, M., and Kalckar, H. M. (1950) Desoxyribose-1-phosphate: I. The phosphorolysis and resynthesis of purine desoxyribose nucleoside. *J. Biol. Chem. 184*, 437–448.
39. Bzowska, A., Kulikowska, E., and Shugar, D. (2000) Purine nucleoside phosphorylases: Properties, functions, and clinical aspects. *Pharmacol. Ther. 88*, 349–425.
40. Ham, A. J., Ranasinghe, A., Koc, H., and Swenberg, J. A. (2000) 4-Hydroxy-2-nonenal and ethyl linoleate form N^2,3-ethenoguanine under peroxidizing conditions. *Chem. Res. Toxicol. 13*, 1243–1250.

41. Lee, S. H., and Blair, I. A. (2000) Characterization of 4-oxo-2-nonenal as a novel product of lipid peroxidation. *Chem. Res. Toxicol. 13*, 698–702.
42. Lee, S. H., Oe, T., and Blair, I. A. (2002) 4,5-Epoxy-2(E)-decenal-induced formation of 1,N^6-etheno-2′-deoxyadenosine and 1,N^2-etheno-2′-deoxyguanosine adducts. *Chem. Res. Toxicol. 15*, 300–304.
43. Chung, F. L., Young, R., and Hecht, S. S. (1984) Formation of cyclic 1,N^2-propanodeoxyguanosine adducts in DNA upon reaction with acrolein or crotonaldehyde. *Cancer Res. 44*, 990–995.
44. Bartsch, H., and Nair, J. (2004) Oxidative stress and lipid peroxidation-derived DNA-lesions in inflammation driven carcinogenesis. *Cancer Detect. Prev. 28*, 385–391.
45. Blair, I. A. (2008) DNA-adducts with lipid peroxidation products. *J. Biol. Chem. 283*, 15545–15549.
46. Delaney, J. C., Smeester, L., Wong, C., Frick, L. E., Taghizadeh, K., Wishnok, J. S., Drennan, C. L., Samson, L. D., and Essigmann, J. M. (2005) AlkB reverses etheno DNA lesions caused by lipid oxidation in vitro and in vivo. *Nat. Struct. Mol. Biol. 12*, 855–860.
47. Ringvoll, J., Moen, M. N., Nordstrand, L. M., Meira, L. B., Pang, B., Bekkelund, A., Dedon, P. C., Bjelland, S., Samson, L. D., Falnes, P. O., and Klungland, A. (2008) AlkB homologue 2-mediated repair of ethenoadenine lesions in mammalian DNA. *Cancer Res. 68*, 4142–4149.
48. Hille, R. (2005) Molybdenum-containing hydroxylases. *Arch. Biochem. Biophys. 433*, 107–116.
49. Krenitsky, T. A., Neil, S. M., Elion, G. B., and Hitchings, G. H. (1972) A comparison of the specificities of xanthine oxidase and aldehyde oxidase. *Arch. Biochem. Biophys. 150*, 585–599.
50. Robins, R. K., Revankar, G. R., Obrien, D. E., Springer, R. H., Novinson, T., Albert, A., Senga, K., Miller, J. P., and Streeter, D. G. (1985) Purine analog inhibitors of xanthine oxidase: Structure activity relationships and proposed binding of the molybdenum cofactor. *J. Heterocycl. Chem. 22*, 601–634.
51. Leonard, N. J., Sprecker, M. A., and Morrice, A. G. (1976) Defined dimensional changes in enzyme substrates and cofactors. Synthesis of *lin*-benzoadenosine and enzymatic evaluation of derivatives of the benzopurines. *J. Am. Chem. Soc. 98*, 3987–3994.
52. Moder, K. P., and Leonard, N. J. (1982) Defined dimensional alterations in enzyme substrates: Synthesis and enzymatic evaluation of some *lin*-naphthopurines. *J. Am. Chem. Soc. 104*, 2613–2624.
53. Obach, R. S., Huynh, P., Allen, M. C., and Beedham, C. (2004) Human liver aldehyde oxidase: Inhibition by 239 drugs. *J. Clin. Pharmacol. 44*, 7–19.
54. Beedham, C. (1987) Molybdenum hydroxylases: Biological distribution and substrate-inhibitor specificity. *Prog. Med. Chem. 24*, 85–127.
55. Jian, W., Lee, S. H., Arora, J. S., Silva Elipe, M. V., and Blair, I. A. (2005) Unexpected formation of etheno-2′-deoxyguanosine adducts from 5(S)-hydroperoxyeicosatetraenoic acid: Evidence for a bis-hydroperoxide intermediate. *Chem. Res. Toxicol. 18*, 599–610.
56. Lee, S. H., Rindgen, D., Bible, R. H., Jr., Hajdu, E., and Blair, I. A. (2000) Characterization of 2′-deoxyadenosine adducts derived from 4-oxo-2-nonenal, a novel product of lipid peroxidation. *Chem. Res. Toxicol. 13*, 565–574.
57. Lee, S. H., Silva Elipe, M. V., Arora, J. S., and Blair, I. A. (2005) Dioxododecenoic acid: A lipid hydroperoxide-derived bifunctional electrophile responsible for etheno DNA adduct formation. *Chem. Res. Toxicol. 18*, 566–578.
58. Pollack, M., Oe, T., Lee, S. H., Silva Elipe, M. V., Arison, B. H., and Blair, I. A. (2003) Characterization of 2′-deoxycytidine adducts derived from 4-oxo-2-nonenal, a novel lipid peroxidation product. *Chem. Res. Toxicol. 16*, 893–900.
59. Beedham, C. (2002) Molybdenum hydroxylases. In *Enzyme systems that metabolise drugs and other xenobiotics* (Ioannides, C., Ed.) pp 147−187, John Wiley & Sons, Ltd., Chichester, U.K.
60. Kitamura, S., Sugihara, K., and Ohta, S. (2006) Drug-metabolizing ability of molybdenum hydroxylases. *Drug Metab. Pharmacokinet. 21*, 83–98.
61. Chen, H. J., and Chang, C. M. (2004) Quantification of urinary excretion of 1,N^6-ethenoadenine, a potential biomarker of lipid peroxidation, in humans by stable isotope dilution liquid chromatography-electrospray ionization-tandem mass spectrometry: Comparison with gas chromatography-mass spectrometry. *Chem. Res. Toxicol. 17*, 963–971.
62. Dutta, S. P., Mittelman, A., and Chheda, G. B. (1980) Metabolism of 1,N^6-ethenoadenosine. *Biochem. Med. 23*, 179–184.

BI801654J